Effect of Tetrahydroquinoline Dyes Structure on the Performance of Organic Dye-Sensitized Solar Cells

Ruikui Chen,[†] Xichuan Yang,*[,†] Haining Tian,[†] Xiuna Wang,[†] Anders Hagfeldt,[‡] and Licheng Sun*[,†,§]

State Key Laboratory of Fine Chemicals, DUT-KTH Joint Education and Research Center on Molecular Devices, Dalian University of Technology, Zhongshan Road 158-46, 116012 Dalian, People's Republic of China, and Center of Molecular Devices, Department of Chemistry, Physical Chemistry, and Center of Molecular Devices, Department of Chemistry, Organic Chemistry, Royal Institute of Technology (KTH), Teknikringen 30, 10044 Stockholm, Sweden

Received March 5, 2007. Revised Manuscript Received May 31, 2007

Eleven novel donor acceptor π-conjugated (D-π-A) organic dyes have been engineered and synthesized as sensitizers for the application in dye-sensitized solar cells (DSSCs). The electron-donating moieties are substituted tetrahydroquinoline, and the electron-withdrawing parts are cyanoacrylic acid group or cyanovinylphosphonic acid group. Different lengths of thiophene-containing conjugation moieties (thienyl, thienylvinyl, and dithieno[3,2-*b*;2′,3′-*d*]thienyl) are introduced to the molecules and serve as electron spacers. Detailed investigation on the relationship between the dye structure, photophysical and photoelectrochemical properties, and performance of DSSCs is described here. The bathochromic shift and increase of the molar extinction coefficient of the absorption spectrum are achieved by introduction of larger conjugation moiety. Even small structural changes of dyes result in significant changes in redox energies and adsorption manner of the dyes on TiO_2 surface, affecting dramatically the performance of DSSCs based on these dyes. The higher performances are obtained by DSSCs based on the rigid dye molecules, **C2** series dyes (Figure 1), although these dyes have lower light absorption abilities relative to other dyes. A maximum solar-to-electrical energy conversion efficiency (η) of 4.53% is achieved under simulated AM 1.5 irradiation (100 mW/cm^2) with a DSSC based on **C2-2** dye (V_{oc} = 597 mV, J_{sc} = 12.00 mA/cm^2, ff = 0.63). Density functional theory (DFT) calculations have been performed on the dyes, and the results show that electron distribution from the whole molecules to the anchoring moieties occurred during the HOMO−LUMO excitation. The cyanoacrylic acid groups or cyanovinylphosphonic acid group are essentially coplanar with respect to the thiophene units, reflecting the strong conjugation across the thiophene-anchoring groups.

1. Introduction

Dye-sensitized solar cells (DSSCs) have become one of the most promising alternatives for the photovoltaic conversion of solar energy as compared to the conventional solid p−n junction photovoltaic devices[1] and are currently undergoing rapid development in an effort to obtain robust, efficient, and cheap devices that are suitable for practical use.[1−4] At the heart of a DSSC system is a mesoporous oxide layer composed of nanometer-sized particles anchored by a monolayer of the charge-transfer dye, especially Ru-polypyridyl-complex.[4] The most widely used sensitizer for the DSSCs has been *cis*-di-(thiocyanato)bis(4,4′-dicarboxy-2,2′-bipyridine) ruthenium(II), coded as N3 or N719 dye depending on whether it contains four or two protons.[5,6] The DSSCs based on ruthenium dye-sensitized nanocrystalline TiO_2 electrodes and liquid redox mediator have already reached solar-to-electrical energy conversion efficiency (η) of up to 11%, which is sufficiently high to be of practical utility.[4] However, the ruthenium dyes that are facing the problem of costs and environmental issues will limit the large-scale application of this type solar cells.

Metal-free dyes, which have many advantages such as large absorption coefficients (attributed to an intramolecular $\pi-\pi^*$ transition), easy molecular design for desired photophysical and photochemical properties, and they are inexpensive and environment friendly,[7c,d] are also adopted as sensitizers for DSSCs. Yet the efficiencies of DSSCs based on metal-free dyes are much lower than that of ruthenium dyes based solar cells in the past decade.[8,9] Recently, performances of DSSCs based on metal-free organic dyes have been remarkably improved by several groups.[7,10−22] A

* Corresponding authors. X.Y., Phone: +86-411-88993886. Fax: +86-411-83702185. E-mail: yangxc@dlut.edu.cn. L.S., Phone: +46-8-7908127. Fax: +46-8-7912333. E-mail: lichengs@kth.se.

† Dalian University of Technology.

‡ Department of Chemistry, Physical Chemistry, Royal Institute of Technology.

§ Department of Chemistry, Organic Chemistry, Royal Institute of Technology.

(1) Grätzel, M. *Nature* **2001**, *414*, 338−344.
(2) Hagfeldt, A.; Grätzel, M. *Acc. Chem. Res.* **2000**, *33*, 269−277.
(3) Special issues on DSSC: *Coord. Chem. Rev.* **2004**, *248*, 1161−1530.
(4) (a) Grätzel, M. *J. Photochem. Photobiol., C* **2003**, *4*, 145−153. (b) Grätzel, M. *Inorg. Chem.* **2005**, *44*, 6841−6851. (c) Grätzel, M. *Prog. Photovolt.: Res. Appl.* **2006**, *14*, 429−442.
(5) Nazeeruddin, Md. K.; Key, A.; Rodicio, I.; Humphry-Barker, R.; Müller, E.; Liska, P.; Vlachopoulous, N.; Grätzel, M. *J. Am. Chem. Soc.* **1993**, *115*, 6382−6390.
(6) Nazeeruddin, Md. K.; Zakeeruddin, S. M.; Humphry-Baker, R.; Jirousek, M.; Liska, P.; Vlachopoulos, N.; Shklover, V.; Fischer, C.-H.; Grätzel, M. *Inorg. Chem.* **1999**, *38*, 6298−6305.

10.1021/cm070617g CCC: $37.00
Published on Web 07/11/2007

much higher solar-to-electrical energy conversion efficiency of up to 9% in full sunlight has been achieved by Ito et al. using an indoline dye.[19] This result suggested that smart engineered metal-free organic dyes are also highly competitive candidates for solar cells due to their low costs and easily synthesis. Furthermore, that metal-free organic dye shows higher performance than ruthenium dyes in solid-state DSSCs makes pure organic dyes extremely interesting for development of cheap and stable DSSCs.[23]

For further development of highly efficient dyes in DSSCs, the dye must be designed to absorb most of the radiation of solar light in visible and near-IR region to produce a large photocurrent response. In addition, suitable energy levels and location of the HOMO and LUMO orbitals of the photosensitizer are required to match the iodine/iodide redox potential and the conduction band edge level of the TiO_2 semiconductor.[24,25] Most of the reported highly efficient metal-free dyes could be classified as electron donor acceptor π-conjugated (D-π-A) compounds. These compounds have been found to possess photoinduced intramolecular charge transfer (PICT) properties,[26] which makes these compounds have broad and intense absorption spectra in the visible region. The charge transfer or separation between the electron donor and acceptor moieties in the molecule may facilitate the rapid electron injection from the dye molecule into the conduction band of the wide band semiconductor, for example, TiO_2, which is required for efficient DSSCs. The cations formed after the electron injection are also a good match to the redox potential of the common used electrolyte, I^-/I_3^-.

We have reported that some tetrahydroquinoline based D-π-A organic dyes show well performance for DSSCs application.[22] It is well known that changes in molecular structure and conjugation system can induce very different optical and physical properties of the D-π-A compounds.[27] To get a better understanding of the relationship between dye structures, photophysical and photoelectrochemical properties, and the performance of DSSCs based on metal-free sensitizers, several series of different D-π-A organic dyes (see Figure 1) have been engineered, synthesized, and fully characterized for the application in DSSCs in this work. These compounds have been constructed based on the novel electron-donating moiety, substituted tetrahydroquinoline. Different types of electron spacers containing thiophene moiety, which is considered to be the ideal constructional unit in dye sensitizer engineering,[7,14−17,20−22] are adopted for expansion of the π-conjugating backbone and adjusting the absorption spectra and HOMO/LUMO levels of the dyes. The dyes which have a C═C bond between/in the spacer and donor parts are denoted as **C1** series, while for the dyes of **C2** series, this C═C bond has been eliminated. For comparison of the donor effects, the *N*-benzyl substituted derivative **C3-1** is also investigated. Most of the dyes have a cyanoacrylic acid group as electron-withdrawing part and for anchoring onto the TiO_2 surface, except for **C4-1** dye, which adopts a cyanovinylphosphonic acid group. The bathochromic shift and increase of the molar extinction coefficient of the absorption spectra are achieved by introduction of a larger conjugation moiety. Even small structural changes of dyes result in significant changes in redox energies and adsorption manner of the dyes on TiO_2 surface, affecting dramatically the performance of DSSCs based on these dyes. Density functional theory (DFT) calculations have been performed on the dyes, and the results show that electron distribution from the whole molecules to the anchoring moieties is occurred during the HOMO−LUMO excitation. The cyanoacrylic acid groups or cyanovinylphos-

(7) (a) Hara, K.; Sayama, K.; Ohga, Y.; Shinpo, A.; Suga, S.; Arakawa, H. *Chem. Commun.* **2001**, 569−570. (b) Hara, K.; Kurashige, M.; Dan-oh, Y.; Kasada, C.; Shinpo, A.; Suga, S.; Sayamaa, K.; Arakawa, H. *New J. Chem.* **2003**, *27*, 783−785. (c) Hara, K.; Tachibana, Y.; Ohga, Y.; Shinpo, A.; Sugab, S.; Sayamaa, K.; Sugiharaa, H.; Arakawa, H. *Sol. Energy Mater. Sol. Cells* **2003**, *77*, 89−103. (d) Hara, K.; Sato, T.; Katoh, R.; Furube, A.; Ohga, Y.; Shinpo, A.; Suga, S.; Sayama, K.; Sugihara, H.; Arakawa, H. *J. Phys. Chem. B* **2003**, *107*, 597−606. (e) Hara, K.; Dan-oh, Y.; Kasada, C.; Ohga, Y.; Shinpo, A.; Suga, S.; Sayama, K.; Arakawa, H. *Langmuir* **2004**, *20*, 4205−4210. (f) Wang, Z.-S.; Hara, K.; Dan-oh, Y.; Kasada, C.; Shinpo, A.; Suga, S.; Arakawa, H.; Sugihara, H. *J. Phys. Chem. B* **2005**, *109*, 3907−3914. (g) Hara, K.; Wang, Z.-S.; Sato, T.; Furube, A.; Katoh, R.; Sugihara, H.; Dan-oh, Y.; Kasada, C.; Shinpo, A.; Suga, S. *J. Phys. Chem. B* **2005**, *109*, 15476−15482. (h) Hara, K.; Miyamoto, K.; Abe, Y.; Yanagida, M. *J. Phys. Chem. B* **2005**, *109*, 23776−23778. (i) Wang, Z.-S.; Cui, Y.; Hara, K.; Dan-oh, Y.; Kasada, C.; Shinpo, A. *Adv. Mater.* **2007**, *19*, 1138−1141.

(8) (a) Ferrere, S.; Zaban, A.; Gregg, B. A. *J. Phys. Chem. B* **1997**, *101*, 4490−4493. (b) Ferrere, S.; Gregg, B. A. *New J. Chem.* **2002**, *26*, 1155−1160.

(9) Jayaweera, P. M.; Kumarasinghe, A. R.; Tennakone, K. *J. Photochem. Photobiol., A* **1999**, *126*, 111−115.

(10) (a) Hara, K.; Horiguchi, T.; Kinoshita, T.; Sayama, K.; Sugihara, H.; Arakawa, H. *Sol. Energy Mater. Sol. Cells* **2000**, *64*, 115−134. (b) Sayama, K.; Tsukagoshi, S.; Hara, K.; Ohga, Y.; Shinpou, A.; Abe, Y.; Suga, S.; Arakawa, H. *J. Phys. Chem. B* **2002**, *106*, 1363−1371.

(11) (a) Hara, K.; Kurashige, M.; Ito, S.; Shinpo, A.; Suga, S.; Sayama, K.; Arakawa, H. *Chem. Commun.* **2003**, 252−253. (b) Hara, K.; Sato, T.; Katoh, R.; Furube, A.; Yoshihara, T.; Murai, M.; Kurashige, M.; Ito, S.; Shinpo, A.; Suga, S.; Arakawa, H. *Adv. Funct. Mater.* **2005**, *15*, 246−252.

(12) Kitamura, T.; Ikeda, M.; Shigaki, K.; Inoue, T.; Anderson, N. A.; Ai, X.; Lian, T.; Yanagida, S. *Chem. Mater.* **2004**, *16*, 1806−1812.

(13) (a) Wang, Z.-S.; Li, F.-Y.; Huang, C.-H. *Chem. Commun.* **2000**, 2063−2064. (b) Wang, Z.-S.; Li, F.-Y.; Huang, C.-H. *J. Phys. Chem. B* **2001**, *105*, 9210−9217.

(14) Thomas, K. R. J.; Lin, J. T.; Hsu, Y. C.; Ho, K. C. *Chem. Commun.* **2005**, 4098−4100.

(15) Tan, S.; Zhai, J.; Fang, H.; Jiu, T.; Ge, J.; Li, Y.; Jiang, L.; Zhu, D. *Chem.-Eur. J.* **2005**, *11*, 6272−6276.

(16) Hagberg, D. P.; Edvinsson, T.; Marinado, T.; Boschloo, G.; Hagfeldt, A.; Sun, L. *Chem. Commun.* **2006**, 2245−2247.

(17) Li, S. L.; Jiang, K. J.; Shao, K. F.; Yang, L. M. *Chem. Commun.* **2006**, 2792−2794.

(18) (a) Horiuchi, T.; Miura, H.; Uchida, S. *Chem. Commun.* **2003**, 3036−3037. (b) Horiuchi, T.; Miura, H.; Uchida, S. *J. Photochem. Photobiol., A* **2004**, *164*, 29−32. (c) Horiuchi, T.; Miura, H.; Sumioka, K.; Uchida, S. *J. Am. Chem. Soc.* **2004**, *126*, 12218−12219.

(19) Ito, S.; Zakeeruddin, S. M.; Humphry-Baker, R.; Liska, P.; Charvet, R.; Comte, P.; Nazeeruddin, Md. K.; Péchy, P.; Takata, M.; Miura, H.; Uchida, S.; Grätzel, M. *Adv. Mater.* **2006**, *18*, 1202−1205.

(20) Kim, S.; Lee, J. K.; Kang, S. O.; Ko, J.; Yum, J.-H.; Fantacci, S.; Angelis, F. D.; Censo, D. D.; Nazeeruddin, Md. K.; Grätzel, M. *J. Am. Chem. Soc.* **2006**, *128*, 16701−16707.

(21) Koumura, N.; Wang, Z.-S.; Mori, S.; Miyashita, M.; Suzuki, E.; Hara, K. *J. Am. Chem. Soc.* **2006**, *128*, 14256−14257.

(22) Chen, R.; Yang, X.; Tian, H.; Sun, L. *J. Photochem. Photobiol., A* **2007**, *189*, 295−300.

(23) Schmidt-Mende, L.; Bach, U.; Humphry-Baker, R.; Horiuchi, T.; Miura, H.; Ito, S.; Uchida, S.; Grätzel, M. *Adv. Mater.* **2005**, *17*, 813−815.

(24) Robertson, N. *Angew. Chem., Int. Ed.* **2006**, *45*, 2338−2345.

(25) Qin, P.; Yang, X.; Chen, R.; Sun, L.; Marinado, T.; Edvinsson, T.; Boschloo, G.; Hagfeldt, A. *J. Phys. Chem. C* **2007**, *111*, 1853−1860.

(26) Yang, J. S.; Liau, K. L.; Wang, C. M.; Hwang, C. Y. *J. Am. Chem. Soc.* **2004**, *126*, 12325−12335.

(27) Marsden, J. A.; Miller, J. J.; Shirtcliff, L. D.; Haley, M. M. *J. Am. Chem. Soc.* **2005**, *127*, 2464−2476.

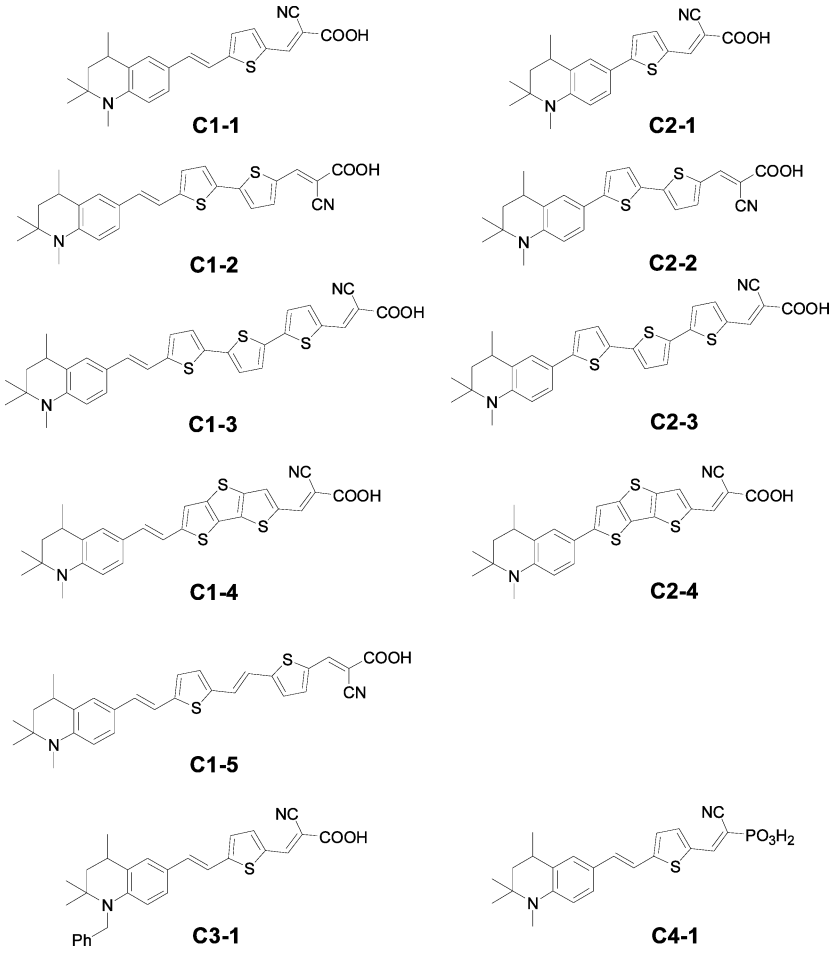

Figure 1. Chemical structures of the tetrahydroquinoline dyes.

phonic acid group are essentially coplanar with respect to the thiophene units, reflecting the strong conjugation across the thiophene-anchoring groups.

2. Experimental Section

Synthesis. Synthesis of the intermediates and sensitizers is described in the Supporting Information in detail.

Analytical Measurements. ^{1}H NMR spectra were recorded with a Varian INOVA 400 NMR instrument. MS data were obtained with GCT CA156 (UK) high-resolution mass spectrometer (HRMS) or HP1100 LC/MSD (USA) mass spectrometer. UV−vis spectra of the dyes in solutions were recorded in a quartz cell with 1 cm path length on a HP 8453 spectrophotometer. Electrochemical redox potentials were obtained by cyclic voltammetry using a three-electrode cell and an electrochemical workstation (BAS100B, USA). The working electrode was a glass carbon electrode, the auxiliary electrode was a Pt wire, and Ag/Ag^+ was used as reference electrode. Tetrabutylammonium hexaflourophosphate ($TBAPF_6$) 0.1 M was used as supporting electrolyte in DMF. Ferrocene was added to each sample solution at the end of the experiments, and the ferrocenium/ferrocene (Fc/Fc^+) redox couple was used as an internal potential reference. The potentials versus NHE were calibrated by addition of 630 mV to the potentials versus Fc/Fc^+.[16]

Fabrication of the Nanocrystalline TiO_2 Solar Cells. Titania paste was prepared from P25 (Degussa, Germany) following a literature procedure[5] and deposited onto the F-doped tin oxide conducting glass (TEC8, sheet resistance of 8Ω/square, Pilkington, USA) by doctor-blading. The resulted layer photoelectrode of 10 μm thickness was sintered at 500 °C for 30 min in air. The sintered film was further treated with 40 mM $TiCl_4$ aqueous solution at 70 °C for 30 min, then washed with water and ethanol, and annealed again at 500 °C for 30 min. After the film was cooled to 80 °C, it was immersed into a dye solution and maintained under dark overnight. The electrode was then rinsed with ethanol and dried. One drop of electrolyte solution was deposited onto the surface of the electrode and penetrated inside the TiO_2 film via capillary action. The electrolyte consists of 0.6 M 1,2-dimethyl-3-propylimidazolinium iodine, 0.1 M LiI, 0.05 M I_2, and 0.5 M 4-*tert*-butylpyridine (TBP) in 3-methoxypropionitrile. A platinized counter electrode was then clipped onto the top of the TiO_2 working electrode to form our test cell.

Photocurrent−Voltage Measurements. The irradiation source for the photocurrent−voltage ($I-V$) measurement is an AM 1.5 solar simulator (16S-002, SolarLight Co. Ltd., USA). The incident light intensity was 100 mW/cm^2 calibrated with a standard Si solar cell. The current−voltage curves were obtained by the linear sweep voltammetry (LSV) method using an electrochemical workstation (LK9805, Tianjing Lanlike Co., China). The measurement of the incident photon-to-current conversion efficiency (IPCE) was performed by a Hypermonolight (SM-25, Jasco Co. Ltd., Japan).

3. Results and Discussion

Synthesis. The structures of the D-π-A tetrahydroquinoline dyes are shown in Figure 1. All of these dyes have been prepared according to several classical reactions, and detailed synthetic procedures are described in the Supporting Information.

Scheme 1. Synthesis Route of Tetrahydroquinoline Containing Functional Groups[a]

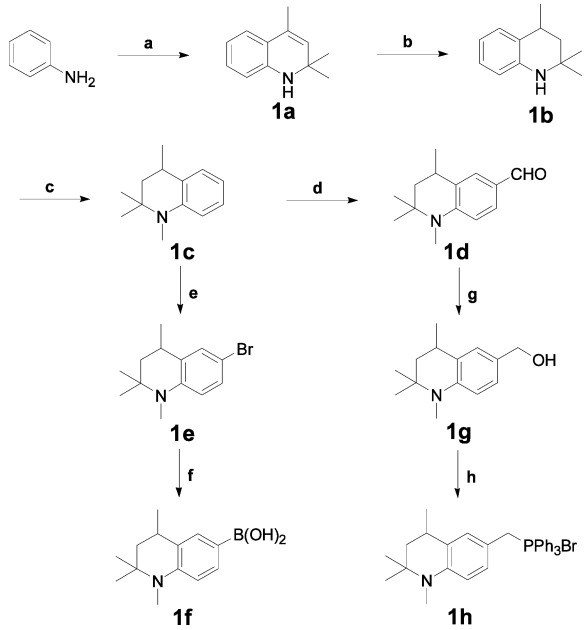

[a] (a) Acetone, *p*-TsOH, cyclohexane, 80−90 °C, 8−10 h, 49%; (b) Raney-Ni, H_2, 1 MPa, 130 °C, 99%; (c) $(CH_3)_2SO_4$, benzene, reflux 2 h, 79%; (d) DMF/$POCl_3$, 55 °C, 6 h, 55%; (e) NBS, CCl_4, rt, 2 h, 93%; (f) (i) *n*-BuLi, THF, −78 °C, 1 h; (ii) $B(OBu)_3$, −78 °C to rt, overnight; (iii) 2% HCl, 68%; (g) $NaBH_4$, alcohol, rt 2 h, 99%; (h) PPh_3HBr, $CHCl_3$, reflux for 3 h, 37%.

The electron-donating moiety tetrahydroquinoline was obtained from aniline as precursor based on improved literature procedures,[28,29] and different functional groups were introduced for subsequent reactions (Scheme 1). For the synthesis of **C1-1** and **C3-1** dyes, the aldehyde precursors **1d** or **3b** were reacted with 2-thienylmethylphosphonate under Wittig−Hornor condition to give intermediates **1i** and **3c**, respectively. Formylation of **1i** and **3c** was achieved by treatment of compounds **1i** or **3c** with 1 equiv of *n*-BuLi, followed by addition of DMF and hydrolysis. The formylated intermediates **1j** and **3d** were reacted with cyanoacetic acid in the presence of piperidine (Knoevenagel condensation reaction) and converted to **C1-1** and **C1-3** dyes, respectively (Scheme S2 in the Supporting Information). For **C2-1** dye, the intermediate **2a** was obtained according to the Suzuki coupling reaction from **1e** and 2-thienylboronic acid, and the **C2-1** dye was synthesized using a procedure similar to the synthesis of **C1-1** or **C3-1** dyes (Scheme S3).

All thiophene π-conjugated spacers **5a**−**8a** were prepared using known procedures. 2,2′-Bithiophene (**5a**) and 2,2′;5′,2″-terthiophene (**6a**) were prepared from 2-bromothiophene or 2,5-dibromothiophene with 2-thienylboronic acid, respectively, under classical Suzuki coupling condition.[30] Dithieno-[3,2-*b*;2′,3′-*d*]thiophene (**7a**) was obtained in three steps from 3-bromothiophene according to the already reported procedures.[31,32] (*E*)-1,2-Bis(5-thienyl)ethane (**8a**) was prepared by McMurry coupling of 2-thiophenecarboxaldehyde.[33] All of these spacers were reacted with 2 equiv of *n*-BuLi and then treated with anhydrous DMF to give the corresponding di-formylated derivatives **5b**−**8b** in good yield. Subsequent mono-Wittig olefination with phosphonium salt **1h** in the presence of potassium carbonate and 18-crown-6-ether led to compounds **5c**−**8c**. After Knoevenagel condensation reaction with cyanoacetic acid, **C1-*n*** ($n = 2-5$) dyes were obtained (Scheme 2).

In the synthesis of **C2-*n*** ($n = 2-4$) dyes, thiophene π-conjugated spacers **5a**−**7a** were subjected to a Vilsmeier reaction in the presence of $POCl_3$ and DMF in refluxing anhydrous 1,2-dichloroethane, affording selectively aldehydes **5d**−**7d**.[34] Subsequent bromination of **5d**−**7d** by NBS gave intermediates **5e**−**7e** in high yield (>95%). Next, these compounds were reacted with **1f** under Suzuki coupling conditions, yielding the formylated derivatives **5f**−**7f**. Corresponded Knoevenagel condensation reactions with cyanoacetic acid gave the target **C2-*n*** ($n = 2-4$) dyes (Scheme S3).

C4-1 dye was prepared by hydrolyzing phosphonate **4a**, which had been obtained from **1j** and diethyl cyanomethylphosphonate, under the presence of trimethylsilane iodide and methanol (Scheme S4).

Absorption, Emission Spectra, and Electrochemical Properties of the Dyes. The absorption spectra of selected dyes in ethanol or DMF solutions are shown in Figure 2, and others are described in the Supporting Information (Figure S2). The characteristic data are collected in Table 1. One can find a strong absorption maximum in the visible region and a relatively weak shoulder in the near UV region, which correspond to the S_1 and S_2 absorption, respectively. In general, the **C1** series dyes, which have C═C bond between/in thiophene-containing spacer and the electron donor, have more bathochromic shifted absorption spectra and larger molar extinction coefficients (ϵ). This result indicates the presence of an ethenyl unit in a photosensitizer could increase the light harvesting efficiency. For the **C1** and **C2** series dyes, the absorption peaks arising from the $\pi-\pi^*$ transition are slightly red-shifted and the ϵ values are increased by the introduction of more thiophene units. For example, the maximum absorption peaks and corresponding ϵ values of **C1-1**, **C1-2**, and **C1-3** are 468 nm (27 500 M^{-1} cm^{-1}), 472 nm (32 900 M^{-1} cm^{-1}), and 475 nm (36 500 M^{-1} cm^{-1}), respectively. The bathochromic shift should be assigned to the extension of π system. Dithieno[3,2-*b*;2′,3′-*d*]thienyl (DTT) moiety has also been introduced into the dye molecules (**C1-4** and **C2-4**) aiming at expansion of the absorption spectra. Yet the maxima of absorption peaks of **C1-4** and **C2-4** dye are nearly the same as those of **C1-1** and **C2-1** dyes, respectively. As compared to the thiophene moiety, the DTT moiety just changes the ϵ value of the dye. In addition, change in the electron donor part has a smaller effect on the absorption feature. Comparing the **C1-1** to the **C3-1** dye, which has the same π-conjugating system

(28) Craig, D. *J. Am. Chem. Soc.* **1938**, *60*, 1458−1465.
(29) Krysin, M. Yu.; Shikhaliev, Kh. S.; Anokhina, I. K.; Shmyreva, Zh. V. *Chem. Heterocycl. Compd.* **2001**, *37*, 227−230.
(30) Miyaura, N.; Yanagi, T.; Suzuki, A. *Synth. Commun.* **1981**, *11*, 513−519.
(31) Janssen, M. J.; Jong, F. De. *J. Org. Chem.* **1971**, *36*, 1645−1648.
(32) Inaoka, S.; Collard, D. M. *J. Mater. Chem.* **1999**, *9*, 1719−1725.
(33) Müller, R. E.; Nord, F. F. *J. Org. Chem.* **1951**, *16*, 1380−1388.
(34) Raimundo, J. M.; Blanchard, P.; Gallego-Planas, N.; Mercier, N.; Ledous-Rak, I.; Hierle, R.; Roncali, J. *J. Org. Chem.* **2002**, *67*, 205−218.

Scheme 2. Synthesis Route of C1-2 to C1-5 Dyes[a]

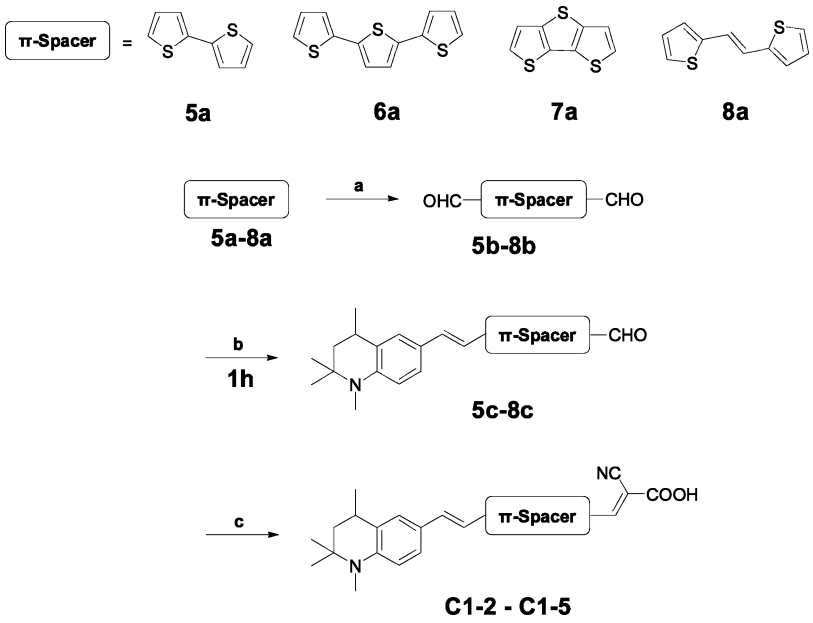

[a] (a) (i) *n*-BuLi, THF, 0 °C to rt for 1 h; (ii) DMF, −78 °C, 1 h; (iii) −78 °C to rt for 2 h; (iv) ice water; (b) **1h**, K_2CO_3, DMF, 18-crown-6-ether, rt for 2 h; (c) cyano-acetic acid, CH_3CN, piperidine, reflux for 2 h.

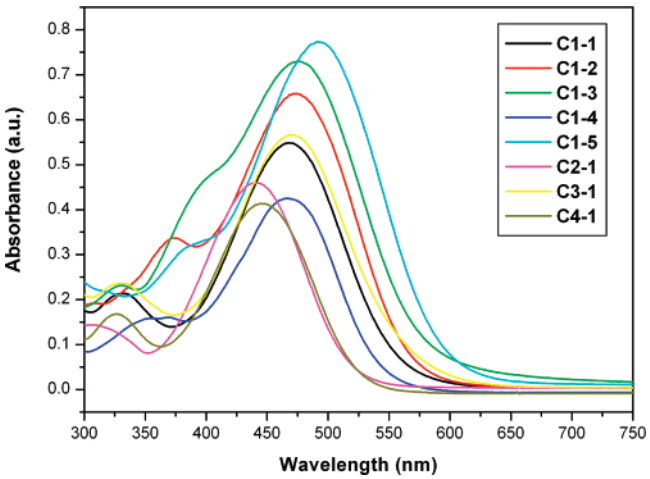

Figure 2. UV−vis spectra of selected dyes in ethanol solutions (2×10^{-5} M) at 25 °C. **C1-4** was measured in DMF solution (2×10^{-5} M) at 25 °C.

and different electron donor moieties, the changes of the absorption peaks and ϵ values are small. When a cyanovinylphosphonic acid group is introduced to the molecule as electron acceptor (**C4-1**), comparing the **C1-1** dye with a cyanoacrylic acid group as electron acceptor, the maximum absorption peak is blue-shifted and the ϵ value is decreased. This is due to the lower electron-withdrawing ability of phosphonic acid group.

When the dyes are attached to TiO_2 surface, the absorption spectra of these dyes are broadened and blue-shifted more or less as compared to that in solutions (Figure 3), indicating strong interactions between the dyes and the semiconductor surface. Also, the strong interactions between the surface and the absorbed molecules often lead to aggregation effects.[35] The blue-shifted values of different dyes are changed obviously depending on the different electron spacer. These values may be results of H-type aggregation of the dyes on TiO_2 surface. Thiophene moiety and ethenyl unit in the molecules could increase the aggregation effect of adsorbed dyes. One can find that the blue-shift values of **C1-1**, **C1-2**, and **C1-3** dyes adsorbed onto TiO_2 surface are 8, 14, and 62 nm, respectively. Additionally, **C1** dyes always have larger blue-shift values as compared to **C2** dyes, indicating that **C1** dyes have a more tendency to aggregate on TiO_2. Many research results have indicated that monolayer dyes anchoring onto TiO_2 surface are necessary for higher efficiency of DSSCs. It seems that more thiophene moieties and also the C═C bond in these dye molecules could lead to higher aggregation, and maybe have a negative effect for DSSCs application. Very recently, this phenomena has been confirmed by Hara et al.;[21] a strategy of introducing alkyl-substitute into thiophene moiety was adopted to reduce the aggregation effect and, thus, gave a higher performance of DSSCs. We also tried to measure the absorbance of dye loaded working electrodes with 10 μm thickness, but the maximum absorbance of all samples was beyond the upper limit of our instrument, indicating >90% of the light harvesting efficiency (LHE) was observed in the main absorbance region of these dye loaded electrodes.[7i]

To get an efficient charge separation, the LUMO of the dye from where the electron injection occurs has to be sufficiently more negative than the conduction band edge of the TiO_2 (E_{cb}), and the HOMO has to be more positive than the redox potential of iodine/iodide. The first oxidation potentials (E_{ox}) corresponding to the HOMO levels of the dyes were measured by cyclic voltammetry (CV) method in DMF solution and are summarized in Table 1. The HOMO levels of the dyes are sufficiently more positive than the iodine/iodide redox potential value, indicating that the oxidized dyes formed after electron injection to TiO_2 could accept electrons from I^- ions thermodynamically. From these values, we can find the introduction of more thiophene units into the molecules shift the HOMO levels negatively, which

(35) Kamat, P. V. *Chem. Rev.* **1993**, *93*, 267−300.

Table 1. Absorption, Emission, and Electrochemical Properties of Dyes

	absorption[a]			emission[a]			
dye	λ_{max} (nm)	ϵ at λ_{max} (M^{-1} cm^{-1})	λ_{max} on TiO_2 (nm)	λ_{max} (nm)	E_{0-0} (V) (abs/em)[d]	E_{ox} (V vs NHE)[e]	$E_{ox} - E_{0-0}$ (V vs NHE)
C1-1	468	27 500	460	647	2.20	0.805	−1.395
C1-2	472	32 900	458[c]	670	2.21	0.732	−1.478
C1-3	475	36 500	413	615	2.30	0.708	−1.592
C1-4[b]	467	21 250	457[c]	643	2.25	0.732	−1.518
C1-5	492	38 700	422	656	2.17	0.721	−1.449
C2-1	441	23 000	437	594	2.38	0.955	−1.425
C2-2	462	33 200	453	652	2.22	0.856	−1.364
C2-3[b]	455	31 100	411	652	2.28	0.806	−1.474
C2-4[b]	444	32 950	437	612	2.36	0.878	−1.482
C3-1	470	28 300	469	635	2.19	0.887	−1.303
C4-1	445	20 660	437	611	2.35	0.725	−1.625

[a] Absorption and emission spectra were measured in ethanol solutions (2×10^{-5} M) at 25 °C. [b] Measured in DMF solutions (2×10^{-5} M) at 25 °C. [c] Obtained by curve fitting method using Origin software (see Figure S12 in the Supporting Information for detail). [d] The zeroth−zeroth transition E_{0-0} value was estimated from the intersection of the absorption and emission spectra. [e] Cyclic voltammetry of the oxidation behavior of the dyes was measured in dry DMF containing 0.1 M tetrabutylammonium hexaflourophosphate ($TBAPF_6$) as supporting electrolyte (working electrode, glassy carbon; reference electrode, Ag/Ag^+ calibrated with ferrocene/ferrocenium (Fc/Fc^+) as an internal reference; counter electrode, Pt).

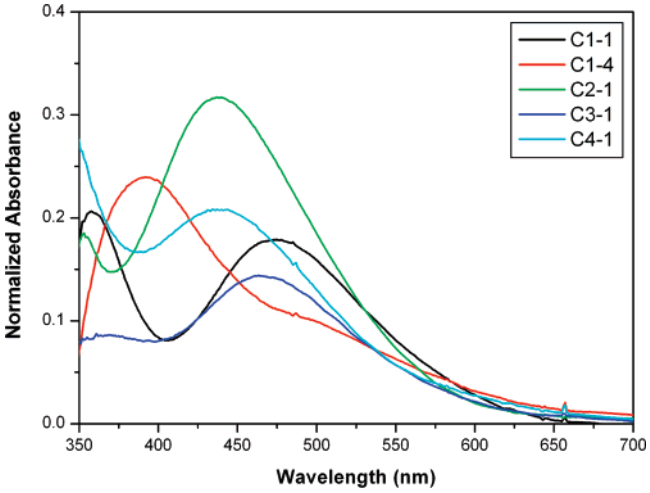

Figure 3. UV−vis spectra of selected dyes attached to TiO_2 surface.

thus decrease the gap between the HOMO level and the redox potential of iodine/iodide. This might reduce the efficiency of regeneration of the oxidized dye by I^- and the overall solar-to-electrical energy conversion efficiency at the same time. The HOMO levels of **C1-1**, **C1-2**, and **C1-3** dyes, which had 1, 2, and 3 thiophene units, were 0.805, 0.732, and 0.708 V (vs NHE), respectively. The C═C bond in the electron spacer also affects the HOMO levels of the dyes. The **C2** series dyes, which eliminate the C═C bond as compared to the **C1** series dyes, have more positive HOMO levels, indicating more efficient electron transfer from the I^- to the oxidized dyes for **C2** series dyes. The changes in the electron donor part and electron acceptor part could also shift the HOMO levels of the dyes. The HOMO levels of **C3-1** and **C4-1** are 0.887 and 0.725 V (vs NHE), respectively, and these values are different with 0.805 V (vs NHE) of **C1-1** dye because of the changes in electron distribution of these dyes.

We consider that the potential levels of the $E_{ox} - E_{0-0}$, where E_{0-0} is the zeroth−zeroth energy of the dyes estimated from the intersection of the absorption and emission spectra, correspond to the LUMO levels of the dyes. These LUMO values are also collected in Table 1, and they are sufficiently more negative than the E_{cb}, −0.5 V vs NHE.[36] The relatively large energy gaps between the LUMO and E_{cb} allow for the addition of the 4-*tert*-butylpyridine (TBP) to the electrolyte, which shift the E_{cb} of the TiO_2 negatively and, consequently, improve the voltage and the total efficiency.[11b]

Table 2. Photovoltaic Performance of DSSCs Based on the Tetrahydroquinoline and N3 Dyes[a]

dye	J_{sc} (mA/cm^2)	V_{oc} (mV)	fill factor (ff)	η (%)
C1-1[b]	8.48	583	0.64	3.17
C1-2	6.99	543	0.62	2.35
C1-3	6.39	521	0.57	1.91
C1-4[c]	6.87	514	0.66	2.34
C1-5	7.22	542	0.59	2.32
C2-1[b]	11.20	600	0.67	4.49
C2-2	12.00	597	0.63	4.53
C2-3[d]	10.00	537	0.64	3.44
C2-4[c]	8.84	522	0.63	2.92
C3-1[b]	9.27	580	0.67	3.61
C4-1	8.54	568	0.67	3.27
N3[e]	14.03	695	0.63	6.16

[a] Conditions: irradiated light, AM1.5 (100 mW/cm^2); TiO_2 films thickness, 10 μm; dye bath, ethanol solutions (1×10^{-4} M) with addition of chenodexoycholic acid (CDCA, 3×10^{-3} M); working area, 0.159 cm^2; electrolyte, 0.6 M 1,2-dimethyl-3-*n*-propylimidazolium iodide/0.1 M LiI/0.05 M I_2/0.5 M 4-*tert*-butylpyridine in 3-methoxyproponitrile. [b] Dye bath: ethanol solution (2×10^{-4} M) with addition of CDCA (3×10^{-3} M). [c] Dye bath: DMF solution (1×10^{-4} M) with addition of CDCA (3×10^{-3} M). [d] Dye bath: DMF solution (1×10^{-4} M). [e] Dye bath: ethanol solution (3×10^{-4} M).

Photovoltaic Performance of DSSCs Based on the Dyes. The photovoltaic properties of the solar cells constructed from these organic dye-sensitized TiO_2 electrodes were measured under simulated AM 1.5 irradiation (100 mW/cm^2). The open-circuit photovoltage (V_{oc}), short-circuit photocurrent density (J_{sc}), fill factor (ff), and solar-to-electrical energy conversion efficiencies (η) are listed in Table 2. Current density−voltage ($J-V$) characteristics and incident photon-to-current conversion efficiencies (IPCE) of devices based on the selected dyes are shown in Figures 4 and 5, respectively. The optimized evaluation conditions for these dyes (except for **C2-3** dye) are determined to be 1×10^{-4} or 2×10^{-4} M of dye in ethanol or DMF solution depending on its solubility, 3 mM chenodeoxycholic acid (CDCA) as a coadsorbent, and the electrolyte is 0.6 M 1,2-dimethyl-3-

(36) Hagfeldt, A.; Grätzel, M. *Chem. Rev.* **1995**, *95*, 49−68.

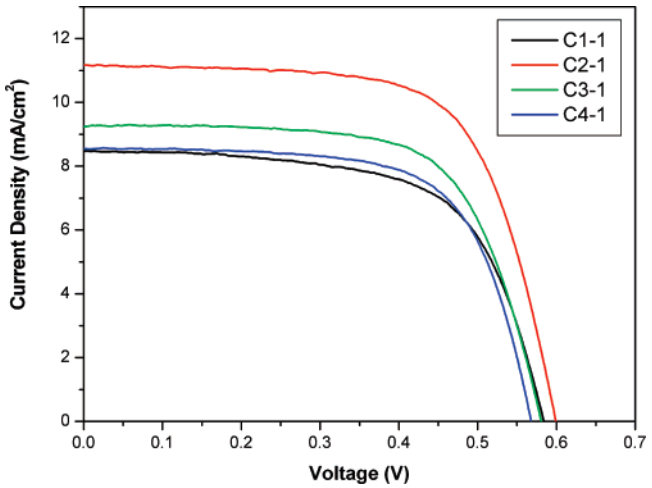

Figure 4. *J*−*V* curves of DSSCs based on selected tetrahydroquinoline dyes.

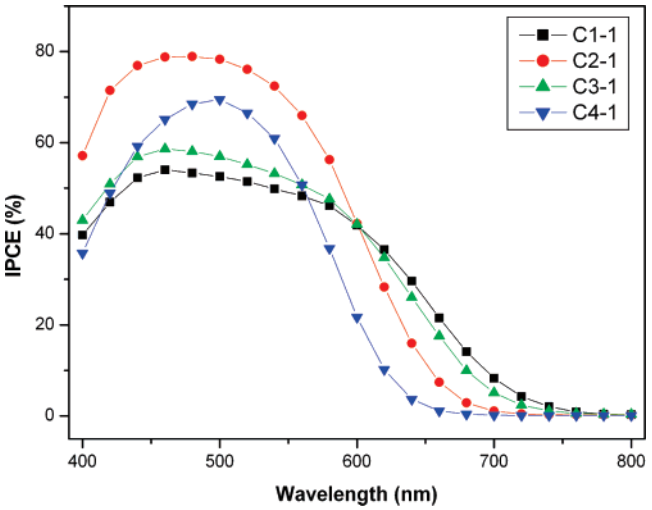

Figure 5. Spectra of incident photon-to-current conversion efficiency (IPCE) for DSSCs based on selected tetrahydroquinoline dyes.

n-propylimidazolium iodide (DMPII)/0.1 M LiI/0.05 M I_2/0.5 M 4-*tert*-butylpyridine in 3-methoxyproponitrile. For **C2-3** dye, a higher η value has been obtained from a TiO_2 film sensitized in the DMF solution of **C2-3** (1×10^{-4} M) without the addition of CDCA. Depending on the different electron spacers, electron donors, and acceptors, these tetrahydroquinoline dyes show distinguishing and interesting results.

In general, the **C2** series dyes give higher IPCE values and energy conversion efficiencies of DSSCs than the corresponding **C1** series dyes, which have a C═C bond in the electron spacer. It seems that the C═C bond is not a suitable constructional moiety for this series of sensitizers getting higher η values, although the C═C bond increases the light harvesting capability. For example, η values of 4.49% (V_{oc} = 600 mV, J_{sc} = 11.20 mA/cm^2, ff = 0.67) and 3.17% (V_{oc} = 583 mV, J_{sc} = 8.48 mA/cm^2, ff = 0.64) were obtained by DSSCs based on **C2-1** and **C1-1** dyes, respectively. The lower performances of DSSCs based on **C1** series dyes are partially due to the lower V_{oc} values, which may be the result of reduced gap between the HOMO levels of **C1** series dyes and redox potential of the I^-/I_3^-. This reduced gap would lead to decreased regeneration efficiency of the

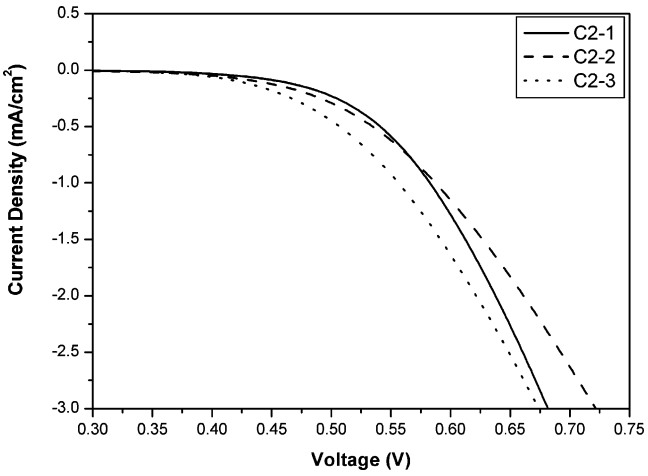

Figure 6. *J*−*V* curves obtained with DSSCs based on **C2-1**, **C2-2**, and **C2-3** dyes under dark condition.

oxidized dye by I^-, and thus result in the increasing of the dark current and the lower performances of the DSSCs. Additionally, **C2** dyes always have higher IPCE values as compared to the corresponding C═C bond containing **C1** dyes (Figures 5, S7). The IPCE is expressed in terms of the LHE, the quantum yield of charge injection (Φ_{inj}), and the efficiency of the collecting the injected charge at the back contact (η_c).[5]

$$\mathrm{IPCE}(\lambda) = \mathrm{LHE}(\lambda) \times \Phi_{inj} \times \eta_c \qquad (1)$$

This means that the **C2** dyes have much higher Φ_{inj} values considering similar unity LHE and η_c values for these dyes. Because J_{sc} can be calculated by integrating the product of the incident photon flux density and the cell's IPCE over wavelengths used for light absorption by the dye,[37] the lower Φ_{inj} and corresponding lower IPCE values will be responsible for the low J_{sc} and performance of **C1** dyes.

The V_{oc} values are decreased with increasing thiophene moiety number, which result in the decrease of the overall efficiency. The V_{oc} values of **C1-1**, **C1-2**, and **C1-3** dyes, which have 1, 2, and 3 thiophene units, are 583, 543, and 521 mV, respectively. The same trend could also be found for **C2-*n*** (n = 1−3) dyes, but the highest J_{sc} value of **C2-2** dye, which could be a result of broadened IPCE response, results in the highest η value of DSSC based on this dye. The *J*−*V* curves obtained under dark conditions for **C2-1**, **C2-2**, and **C2-3** dyes are shown in Figure 6. It is found that the onsets for **C2-1** and **C2-2** dyes are similar but more positive than **C2-3** dye. This indicates that the back-electron-transfer process corresponding to the reaction between the conduction-band electrons in the TiO_2 and I_3^- in the electrolyte under dark conditions occurs more easily in DSSCs based on dyes with more thiophene units. The electron recombination at the interfaces will directly lead to lower V_{oc} values.[7h] In addition, as discussed in the UV−vis section, more thiophene moieties result in more aggregation of dyes. So, a suitable electron spacer should be adopted to the sensitizer structure for the balance of the V_{oc} and J_{sc} values, thus giving the highest η value.

(37) Tachibana, Y.; Hara, K.; Sayama, K.; Arakawa, H. *Chem. Mater.* **2002**, *14*, 2527−2535.

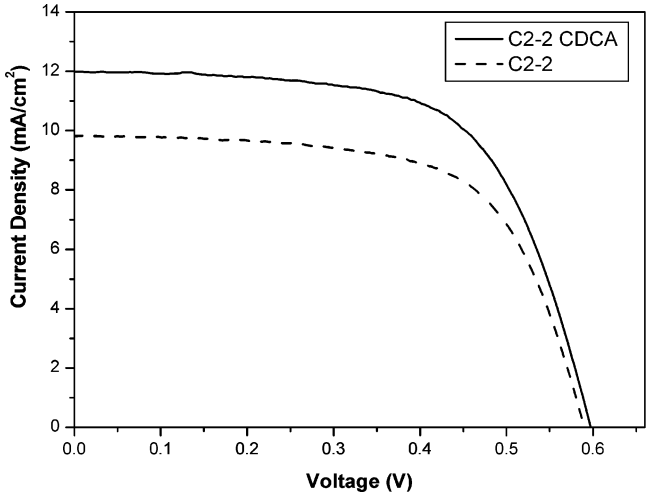

Figure 7. $J-V$ curves of DSSCs based on **C2-2** dye with (−) or without (- - -) the addition of CDCA (3×10^{-3} M) into dye bath.

The changes in the electron donor (**C3-1**) or acceptor moiety (**C4-1**) of the dyes, as compared to **C1-1** dye, give higher performances of DSSCs. The **C3-1** and **C1-1** dyes have even the same absorption abilities, but give much different η values of DSSCs. This would be the result of the broadened and increased IPCE response (Figure S7) of **C3-1** dye, which gives a higher J_{sc} value and, thus, higher η value. The **C4-1** dye, where the carboxylic acid group in **C1-1** is replaced by a phosphonic acid group, has higher IPCE values in the visible light region and also results in a higher η value, indicating the phosphonic acid group is also a suitable anchoring group for DSSCs getting high efficiency.

When chenodexoycholic acid (CDCA, 3×10^{-3} M) was added to the dye bath as a coadsorbent to prevent aggregation, much higher photovoltaic performances were achieved, except for **C2-3** dye (Table S1 and Figure S8). This result indicates that these organic dyes have more or less aggregation conformation on TiO_2 surface, as observed in the UV−vis section. After the addition of CDCA to the dye bath, the overall conversion efficiency of DSSCs based on **C2-2** dye was 4.53%, relative to the lower value of 3.74% obtained by a DSSC based on this dye without the addition of CDCA in the dye bath (Figure 7). However, for **C2-3** dye, pure dye solution (1×10^{-3} M in DMF) sensitized TiO_2 electrode give a higher η value of 3.44% ($V_{oc} = 537$ mV, $J_{sc} = 10.00$ mA/cm^2, ff = 0.64) of a DSSC. The reason for this might be the different aggregation and anchoring manner of the dyes in DMF and other solutions. We also tried to make dye-sensitized TiO_2 electrodes from DMF solutions of other tetrahydroquinoline dyes, but ethanol solutions of most of the tetrahydroquinoline dyes give better results.

It is interesting to note that the higher η values are obtained based on the **C2** series dyes, which have the lowest light absorption ability relative to other dyes. One reason for **C2** series dyes getting higher performance could be the elimination of the C═C bond in the dye structure and adoption of suitable electron spacer. In a previous study, Yang et al.[38] have indicated that the excited state of some C═C bond containing compounds adopts a twisted intramolecular charge-transfer geometry. This twisting process is also observed for a similar molecule where the carboxylate group in **C1-1** is replaced by a phosphonate group.[39] One assumption to explain the low performance of C═C bond containing dyes would be the existence of the similar twisting process, which leads to the possible trans−cis photoisomerization. The geometric change in the excited state might decrease the excited-state energy of these dyes and result in a less efficiency of electron injection. We attempted to synthesize sensitizer without C═C bond and larger π-conjugating system (**C2-4** dye), aiming at enhancing the absorption ability of the dye and the overall conversion efficiency. Unfortunately, the result is negative because of the very low V_{oc} and J_{sc} values of DSSC based on **C2-4** dye. The aggregation of **C2-4** dye on TiO_2 surface or not a full optimization of the evaluation conditions for this dye may be the reason for this lower DSSC performance.

Although efficiencies of up to 11% have been obtained by DSSCs based on N3 dye, under the conditions in our lab, the η value of a DSSC based on N3 dye is 6.16%. A DSSC gave the highest η value of 4.53% based on **C2-2** dye under the same condition. The lower performance of the DSSCs based on these tetrahydroquinoline dyes is probably due to the narrow action spectra in the whole solar spectrum. The onset wavelengths of the IPCE spectra for DSSCs based on these dyes are about 700−760 nm (Figures 5 and S7). Only for **C2-1** and **C2-2** dyes, IPCE values higher than 70% are observed in the ranges of 430−540 nm and 460−500 nm, respectively, which help them to give a higher performance of DSSCs among these dyes. Although the highest IPCE value (75%) of **C2-2** dye is lower than that (79%) of **C2-1** dye based DSSCs, the broadened action spectrum of **C2-2** dye results in a better performance of DSSC. This indicates that dyes with rigid molecular structure and larger π-conjugating backbone should be paid much attention to improve the solar cell performance.

Molecular Orbital Calculations. To get an insight into the molecular structure and electron distribution of the organic dyes, all of the dyes geometries have been optimized using DFT calculations with Gaussian 03 program.[40] The calculations were performed with the B3LYP exchange-correlation functional[41] under 6-31+G(d) basis set.[42] The electron distribution of the HOMO and LUMO of the selected dyes is shown in Figure 8. It reveals that the cyanoacrylic acid groups or cyanovinylphosphonic acid group are essentially coplanar with respect to the thiophene units, reflecting the strong conjugation across the thiophene-acceptor groups.[20] We also notice that the HOMO−LUMO excitation induced by light irradiation could move the electron distribution from the whole molecules to the anchoring moieties. Assuming similar molecular orbital geometry when anchored to TiO_2, the position of the LUMO

(38) Yang, J. S.; Liau, K. L.; Hwang, C. Y.; Wang, C. M. *J. Phys. Chem. A* **2006**, *110*, 8003−8010.

(39) Chen, R.; Zhao, G.; Yang, X.; Jiang, X.; Liu, J.; Tian, H.; Gao, Y.; Liu, X.; Han, K.; Sun, M.; Sun, L. *J. Mol. Struct.*, doi: 10/1016/j.molstruc.2007.05.045.

(40) Frisch, M. J.; et al. *Gaussian 03*, revision B.03; Gaussian, Inc.: Pittsburgh, PA, 2003.

(41) Beche, A. D. *J. Chem. Phys.* **1993**, *98*, 5648−5652.

(42) Ditchfield, R.; Herhe, W. J.; Pople, J. A. *J. Chem. Phys.* **1971**, *54*, 724.

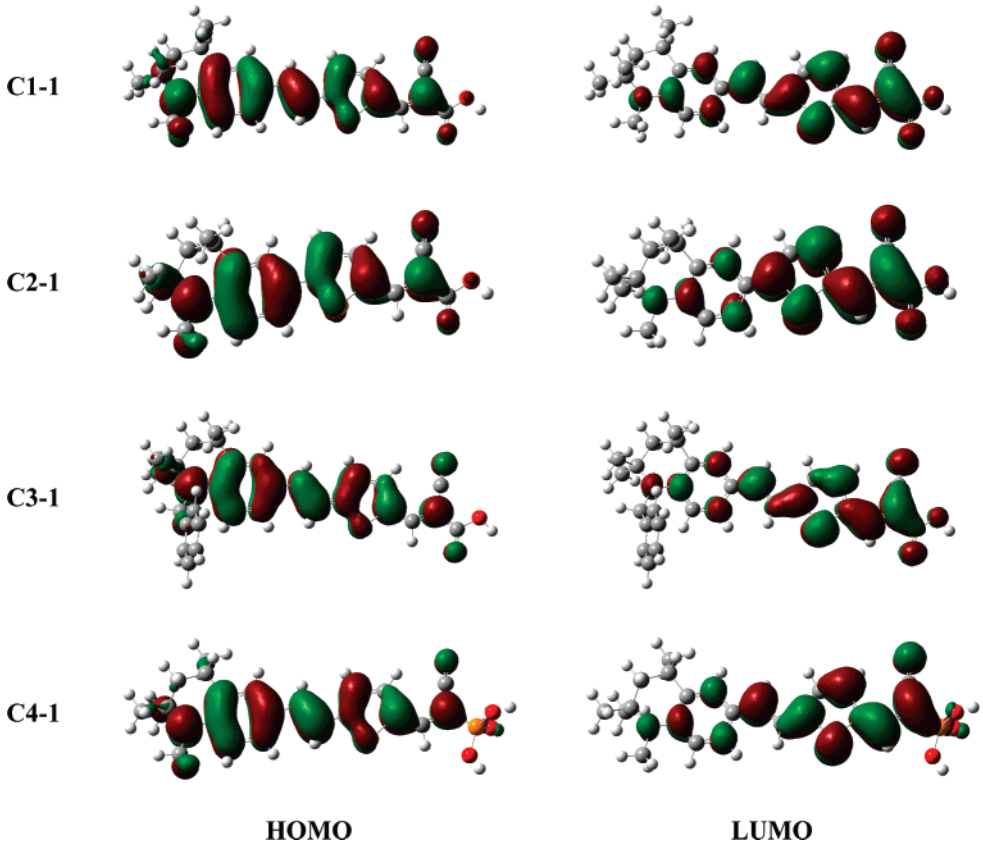

Figure 8. The frontier orbitals of the selected tetrahydroquinoline dyes optimized at the B3LYP/6-31+G(d) level.

close to the anchoring groups will enhance the orbital overlap with the titanium 3d orbitals and thus favor electron injection from dye to TiO_2.[16]

4. Conclusion

Eleven novel pure D-π-A organic dyes have been engineered and synthesized as photosensitizers for DSSC applications. The electron-donating moieties are substituted tetrahydroquinoline, and the electron-withdrawing parts are cyanoacrylic acid or cyanovinylphosphonic acid groups. Different lengths of thiophene-containing conjugation moieties (thienyl, thienylvinyl, and dithieno[3,2-*b*;2′,3′-*d*]thienyl) are indroduced to the molecules and serve as electron spacers. The bathochromic shift and increase of the molar extinction coefficient of the absorption spectrum are achieved by introduction of a larger conjugation moiety. Even small structural changes of dyes result in significant changes in redox energies and adsorption manner of the dyes on TiO_2 surface, affecting dramatically the performance of DSSCs based on these dyes. The elimination of C═C bond and adoption of suitable electron spacers in dye structures are useful for getting higher η values of DSSCs based on these dyes. The rigid dye molecules, **C2** series, give the higher efficiencies of DSSCs, although these dyes have lower light absorption capabilities relative to other dyes. A maximum η value of 4.53% is achieved under simulated AM 1.5 irradiation (100 mW/cm^2) with a DSSC based on **C2-2** dye (V_{oc} = 597 mV, J_{sc} = 12.00 mA/cm^2, ff = 0.63). Under the same conditions, the η value of a DSSC based on N3 dye is 6.16%. DFT calculations have been performed on the dyes, and the results show that electron distribution from the whole molecules to the anchoring moieties occurred during the HOMO−LUMO excitation. The cyanoacrylic acid groups or cyanovinylphosphonic acid group are essentially coplanar with respect to the thiophene units, reflecting the strong conjugation across the thiophene-anchoring groups. Our results suggest that a rigid molecular structure as well as a suitable larger π-conjugating system are helpful for dyes getting higher solar-to-electricity conversion efficiencies in DSSCs.

Acknowledgment. The Program of Introducing Talents of Discipline to Universities supports this work. We thank the National Natural Science Foundation of China (grant no. 20633020), the Ministry of Science and Technology (MOST), Ministry of Education (MOE), the Swedish Energy Agency, the K&A Wallenberg Foundation, and the Swedish Research Council for financial support. We would also like to thank Prof. Songyuan Dai at the Institute of Plasma Physics, CAS, China, for kind help with the solar cell test. We are also grateful to Tannia Marinado and Daniel P. Hagberg at the Royal Institute of Technology, Sweden, and Dr. Hongguang Cui at DUT for helpful discussion.

Supporting Information Available: Synthetic schemes leading to the preparation of the dyes used in this study and related analytical data. Photophysical data of the dyes and characterization of dye-sensitized solar cells based on these dyes. Full ref 38 (PDF). This material is available free of charge via the Internet at http://pubs.acs.org.

CM070617G